Received: 20 April 2022 | Revised: 22 August 2022 | Accepted: 30 August 2022

DOI: 10.1111/ppl.13776

UPTAKE, TRANSPORT AND ASSIMILATION

Physiologia Plantarum

Cytokinins as boron deficiency signals to sustain shoot development in boron-efficient oilseed rape

Benjamin Pommerrenig[1,2] | Maximilian Faber[1] | Mohammad-Reza Hajirezaei[1] | Nicolaus von Wirén[1] | Gerd Patrick Bienert[1,3]

[1]Department of Physiology and Cell Biology, Leibniz Institute of Plant Genetics and Crop Plant Research (IPK), Gatersleben, Germany

[2]Plant Physiology, University Kaiserslautern, Kaiserslautern, Germany

[3]Crop Physiology, TUM School of Life Sciences, Technical University of Munich, Freising, Germany

Correspondence
Gerd Patrick Bienert, Crop Physiology, TUM School of Life Sciences, Technical University of Munich, Alte Akademie 12, Freising 85354, Germany.
Email: patrick.bienert@tum.de

Funding information
Deutsche Forschungsgemeinschaft, Grant/Award Numbers: 1668/1-1, 1668/1-2

Edited by J.K. Schjørring

Abstract

Boron (B) deficiency is a highly prominent nutrient disorder. While B-efficient accessions have recently been identified in the highly B-demanding crop oilseed rape, it remained unclear which physiological processes underlie B efficiency and which signaling pathways trigger an efficient B-deficiency response. Here, we compared, under three different B supply conditions, two *Brassica napus* accessions with contrasting B efficiency. Shoot biomass formation, B distribution patterns and metabolic dynamics of different phytohormone species were studied using a combination of mass spectrometry-based analyses and physiological measurements. Our results show that the B-efficient accession *CR2267* does not differ from the B-inefficient accession *CR2262* in terms of B accumulation and subcellular B-partitioning, although it displays no morphological B-deficiency symptoms under severe B-deficient conditions. Investigating phytohormone metabolism revealed a strong accumulation of cytokinins in *CR2267* at a developmental stage when striking B-dependent differences in biomass and organ formation emerge in the two *B. napus* accessions. In contrast, elevated levels of the stress hormone abscisic acid as well as bioactive auxins, representing functional antagonists of cytokinins in shoots, were detected only in *CR2262*. Our results indicate that superior B efficiency in *CR2267* relies on a higher B utilization efficiency that builds on an earlier and higher cytokinin biosynthesis required for the maintenance of the shoot meristem activity and proper leaf development. We further conclude that an elevated abundance of cytokinins is not a consequence of better plant growth but rather a presumption for better plant growth under low-B conditions.

1 | INTRODUCTION

Boron is an essential element for vascular plants (Marschner, 2012; Warington, 1923; Wimmer et al., 2020). The only well-established biochemical function of B with physiological relevance for plants is its role in maintaining the integrity of cell walls. Boron forms di-ester bonds with apiose residues of the polysaccharide rhamnogalacturonan II (RG-II), thereby crosslinking two RG-II monomers in the cell wall's pectin layer (O'Neill et al., 2004). These RG-II-B-RG-II complexes serve as space holders between cellulose fibers and add porosity and flexibility to the tight mesh formed by the remaining pectin

This article is dedicated to Dr Kai Eggert, IPK Gatersleben, who significantly contributed to this study but deceased on August 13, 2018.

This is an open access article under the terms of the Creative Commons Attribution License, which permits use, distribution and reproduction in any medium, provided the original work is properly cited.
© 2022 The Authors. *Physiologia Plantarum* published by John Wiley & Sons Ltd on behalf of Scandinavian Plant Physiology Society.

compounds (Fleischer et al., 1999; Kobayashi et al., 1996; Ryden et al., 2003). Despite the obvious fact that B is an essential micronutrient, the exact molecular function of B in vegetative and reproductive development is far from being understood (Lewis, 2019; Wimmer et al., 2020). Moreover, little is known about mechanisms involved in the qualitative or quantitative perception of the absence or presence of this nutrient, and information on regulatory mechanisms adjusting plant metabolism and development to overcome low or excessive B conditions are scarce to date. It has been shown that the promoter activity of *AtNIP5;1*, encoding a B channel of crucial importance for B nutrition in Arabidopsis, which is rapidly and highly upregulated under B-deficient growth conditions (Takano et al., 2006), is also significantly altered in response to phytohormones such as abscisic acid (ABA), ethylene, auxin, or cytokinin (CK) treatments independent of the B nutritional status of the plants (Gómez-Soto et al., 2019). This observation suggests that phytohormones play an important signaling role in early B deficiency responses. Phytohormones are essential signaling molecules in plants governing the regulation of growth and development and have been additionally demonstrated to be crucial regulators of response reactions to abiotic stress conditions, including a few nutrient deficiencies (Jia et al., 2019; Koprivova & Kopriva, 2016; Rubio et al., 2009; Sultan, 2000; Wolters & Jurgens, 2009). The general lack of knowledge on how plants regulate their B nutritional status is surprising since plants drastically reduce apical shoot and root meristem activity under B-limiting conditions, resulting in rapid inhibition of above- and below-ground growth. Moreover, B deficiency has a yet not understood impact on cell and tissue differentiation. These all are processes in which phytohormones play crucial signaling and regulatory roles. Among all crop species, *B. napus* belongs to those with the highest demand for B (Gupta, 1980). For proper seedling vigor and grain yield production in *B. napus*, adequate B supply from the soil is indispensable (Eggert & von Wirén, 2015; Goldbach et al., 2001). Knowledge on physiological mechanisms and genetic factors driving B efficiency is therefore urgently needed to reduce B deficiency-caused yield losses and to develop B-efficient elite accessions for sustainable agriculture. In this context, it is highly important to understand (1) whether and how phytohormone action contributes to B efficiency and (2) which cross talks exist between phytohormone metabolism and mechanisms regulating the B nutritional status.

To date, quantifications of single phytohormone species and expression analyses of genes involved in phytohormone biosynthesis, degradation or signaling together with reverse genetic approaches exploiting plant genotypes with modified expression of phytohormone-related genes successfully identified phytohormone actions, regulatory metabolic networks and molecular signaling cascades that trigger plant responses to nutrient deficiencies (Jia et al., 2019; Koprivova & Kopriva, 2016). In a showcase for nutrient-dependent plant responses, Eggert and von Wirén (2017) explored and quantified synergistic and antagonistic shifts in phytohormone species patterns induced by different B supply levels to *B. napus* plants. It was shown that the B-dependent growth response was closely associated with de-novo synthesis of CKs and the rerouting of inactive toward active forms of CKs. In addition, gibberellin species from the non-13-hydroxylation pathway increased continuously with B supply, whereas the brassinosteroid castasterone paralleled shoot growth primarily at suboptimal B nutrition. These results indicated that the B nutritional status is closely linked to growth responses via the biosynthesis and metabolism of growth-promoting phytohormones. However, it remained open whether phytohormone homeostasis strictly reflects the B nutritional status.

The few studies measuring B-dependent phytohormone responses in *B. napus* or other plants have in common that they focused either on early developmental stages, i.e., before the first true leaves appear, or that phytohormone levels were analyzed only at a single time point. Consequently, these studies took only a snapshot of a temporally dynamic metabolic phytohormone network. Within the present study, we monitored phytohormone levels in recently identified B-efficient and B-inefficient accessions (Pommerrenig, Junker, et al., 2018) grown under varied B nutritional states from the seedling to the first true leaf stage wit. Importantly, at the latter stage, striking differences in biomass and organ formation between the two *B. napus* accessions emerged already.

The major goals of this study were therefore to (1) monitor simultaneous dynamics of phytohormone metabolism during seedling establishment, (2) determine developmental-dependent changes in phytohormone species in response to the B nutritional status and their association with B-dependent growth responses, and (3) identify differential phytohormone responses to B deficiency in a B deficiency-sensitive and -tolerant accession that may underlie B efficiency mechanisms.

2 | MATERIALS AND METHODS

2.1 | Plant material

Brassica napus accessions *CR2267* and *CR2262* were obtained from the *B. napus* seed collection of the IPK Genebank (https://gbis.ipk-gatersleben.de/gbis2i/). Passport data of used accessions are accessible online via the Genebank Information System of the IPK Gatersleben, GBIS/I (https://gbis.ipk-gatersleben.de/gbis2i/).

2.2 | Plant growth conditions

Rapeseed plants were germinated and grown in pots (⌀16 cm) filled with 1 kg of soil substrate in the greenhouse. Greenhouse conditions were set to long-day conditions (16 h day/8 h night) at 22/18°C, 60/70% relative humidity, and 250 μmol photons PAR m^{-2} s^{-1} light intensity. Soil substrate consisted of "Fruhstorfer Nullerde" added with 0.5% $CaCO_3$ and 0.3% CaO. Calcium concentration was adjusted by mixing 20 kg soil with 1 L of $CaCO_3$ (100 g L^{-1}) and 1 L of CaO (60 g L^{-1}) in a cement mixer for 10 min. Plants were watered every 2 days with 250 ml per pot with a 1x Hoagland-like nutrient solution containing either 2 mM (B2; B surplus conditions; high), 200 μM

(B1; B-sufficient conditions; medium) or 0 μM boric acid (B0; B-deficient conditions; low). All solutions additionally contained: 7.5 mM NH_4NO_3, 2.9 mM KH_2PO_4, 850 μM $MgSO_4$, 340 μM K_2SO_4, 320 μM $MnCl_2$, 52 μM $CuSO_4$, 20 μM NaFeEDTA, 4.5 μM $ZnSO_4$, and 0.4 μM $NaMoO_4$. Nutrient solutions were prepared out of 100x stock solution mixes with ultrapure water. 100x stock solution mixes were prepared in 1 L plastic bottles (Nalgene): 100x macro-element mix (60 g L^{-1} NH_4NO_3, 40 g L^{-1} KH_2PO_4, 20 g L^{-1} $MgSO_4$, 6 g L^{-1} K_2SO_4), 100x microelement mix (4 g L^{-1} $MnCl_2$, 1.3 g L^{-1} $CuSO_4 \times 5H_2O$, 1.3 g L^{-1} $ZnSO_4 \times 7H_2O$, 8.5 mg L^{-1} $NaMoO_4$), 100x NaFeEDTA mix (0.7 g L^{-1}). About 30 seedlings were germinated in one pot. At 10 days after germination (DAG), the seedling number per pot was reduced to five. No glassware was used in any process during the preparation of the nutrient solution or the irrigation of the plants.

Plants were harvested on 5, 10, 15, 20, and 25 DAG in four biological replications per accession and treatment. For each biological replicate, 15–20, 7–9, 5–7, 3–5, and 1–3 aerial parts of plants (hereupon referred to as shoots or shoot material) were pooled at 5, 10, 15, 20, and 25 DAG, respectively. Shoot material was frozen in liquid nitrogen and the fresh weight was determined. After freeze-drying the samples for 72 h, the dry weight (DW) was determined. Dry material was homogenized in a mixer mill (MM200; Retsch) with steel balls (90 s and 125 Hz) and stored at −80°C.

2.3 | Extraction of the water-soluble, pectin-bound, and non-soluble shoot B fractions

Water-soluble B fraction: 50–100 mg of shoot material were mixed with 80% ethanol (pre-cooled to −20°C) for 15 min at 4°C. The suspension was then sonicated for 5 min at 4°C. The sample was centrifuged at 20,817*g*, 4°C, 10 min. The pellet was re-extracted three times and the supernatants (S1) were pooled. The pellet was washed with 1.5 ml acetone, 15 min, 25°C, sonicated for 5 min at 4°C, and centrifuged at 20,817*g*, 4°C, 10 min. The supernatant (S2) was combined with S1. Then, the pellet was washed with 1.5 ml methanol, 15 min, 25°C, sonicated for 5 min at 4°C, and centrifuged at 20,817*g*, 4°C, 10 min. S1, S2, and S3 were combined, the solvents, and water were evaporated in a Speed Vac at 60°C. Subsequently, the dried extract was digested in 2 ml HNO_3 and analyzed by HR–ICP–MS analysis.

Pectin-bound B fraction (acid-soluble pectin fraction): the remaining colorless pellet from the extraction of the water-soluble B fraction was washed with 1.5 ml water, 2% acetic acid, for 15 min at 80°C, sonicated for 5 min, and centrifuged at 20,817*g*, 25°C, 10 min. This procedure was repeated three times. Pooled supernatants were dried in a Speed Vac 60°C. The pectin fraction was digested in 2 ml HNO_3 and analyzed by HR–ICP–MS analysis.

Water-insoluble B fraction: the remaining pellet (containing the alkali-soluble pectin fraction, hemicellulose, and cellulose) from the extraction of the pectin-bound B fraction was dried at 105°C for 3 h, digested in 10 ml HNO_3 and analyzed by HR–ICP–MS analysis.

2.4 | Extraction and measurement of soluble amino acids

Soluble amino acids were measured as described in Zierer et al. (2016). At least 10 mg of dry material was used for the analysis.

2.5 | Extraction and measurement of soluble sugars

Soluble sugars were measured as described in Hajirezaei et al. (2000).

2.6 | HR–ICP–MS analysis of boron and calcium

Ten to twenty milligrams of dry matter were digested using a high-performance microwave reactor (UltraClave IV; MLS GmbH). Nitric acid (HNO_3) 65% Suprapur, hydrogen peroxide and sulfuric acid (Merck) were used for microwave digestion. ^{11}B was used as external element standard and ^{103}Rh as internal element standard. Both were prepared from certified reference material from CPI-International. The analysis of B was performed with a sector field high-resolution ICP–MS (Element 2, Research Thermo Fisher Scientific) using software v.3.1.2.242 (Eggert & von Wirén, 2013).

2.7 | Extraction of phytohormones

Phytohormones were extracted by the following procedures. For auxins, ABA, SA, and CKs, about 25 mg of freeze-dried and ground shoot material was sequentially extracted by methanol/water under acidic and basic conditions. All protocols are described in detail in Eggert and von Wirén (2017). For auxins, ABA, SA, and CKs, 25 mg dry matter were transferred into 2 ml Eppendorf tubes, to which two steel balls and 750 μl cold 0.1% formic acid (FA) solution were added. The suspension was mixed for 30 s, sonicated for 2 min at 4°C, and extracted in an overhead shaker for 15 min at 4°C. Samples were then centrifuged for 10 min at 4°C and 17,500 g force and the supernatant was transferred to a new Eppendorf tube. The pellet was re-extracted and both supernatants were combined. To each combined supernatant, 50 μl of an internal standard mix was added. The supernatant was then added to an 1 cc/30 mg HLB cartridge (Waters), which was preconditioned with 1 ml MeOH containing 0.1% FA and equilibrated with 2 × 1 ml 0.1% FA. The HLB cartridge was washed twice with 1 ml 0.1% FA and eluted with 2 × 600 μl 90% MeOH containing 0.1% FA. Then, MeOH was evaporated using a vacuum centrifuge, and the residue was resuspended in 1 ml 0.1% FA and sonicated at 4°C for 2 min. In the second solid phase extraction step, acidic and neutral compounds (ABA, auxins, SA) were separated from the basic CKs using a 1 cc/30 mg MCX cartridge (Waters). The MCX cartridge was preconditioned with 1 ml MeOH containing 0.1% FA and equilibrated with 2 × 1 ml 0.1% FA. Samples were then added to the column and washed twice with 1 ml 0.1%

FA. Acidic and neutral compounds were eluted with 2 × 600 μl 100% MeOH. For the elution of CKs, 1 × 600 μl 60% MeOH containing 5% ammonium and 1 × 600 μl 60% acetonitrile containing 5% ammonium were used. Samples were evaporated in a vacuum centrifuge to dryness, resolved in 10 μl 50% MeOH containing 0.5% FA, vortexed for 30 s and sonicated for 2 min, filled up to 50 μl with H_2O and transferred to a glass vial for analysis.

2.8 | LC–MS–MS analysis

LC–MS–MS analysis was performed as described in Eggert and von Wirén (2017). Ten microliters of purified extracts from the shoots of seedlings were injected into an ultra-performance LC system (Acquity) coupled with a Xevo TQ mass spectrometer (Waters). The sample analytes were separated on an Acquity UPLC BEH C18 1.7-lm, 2.1 9100 mm column coupled with a VanGuard pre-column BEH C18 1.7 lm, 2.1 9 5 mm. The column temperature for all methods was set to 40°C. The autosampler temperature was set to 4°C for auxins, ABA, SA, and CKs.

For LC, the used mobile phases were 0.1% FA (A) and 0.1% FA in MeOH (B). The flow was set to 0.4 ml min^{-1}. The gradient conditions for auxin, ABA, and SA analysis were as follows: A, 90% in 0–0.3 min; 90–80% in 0.3–0.7 min; 80–40% in 0.7–8 min; 40–1% in 8–8.5 min; 1% in 8.5–8.9 min; 1–90% in 8.9–9.0 min; and 90% in 9.0–10.0 min. The gradient conditions for CK analysis were as follows: A, 95% in 0–0.5 min; 95–90% in 0.5–1.0 min; 90–85% in 1.0–2 min; 85–1% in 2–8.0 min; 1% in 8.0–8.9 min; 1–95% in 8.9–9.0 min; and 95% in 9.0–10.0 min. The Xevo TQ MS was operated in both ESI+ and ESI− ion modes. The electrospray capillary voltage was 2.45 kV for auxins, ABA, SA, and CKs with a cone voltage of 20 V. The cone and desolvation gas flows were set to 20 and 1000 L h^{-1}. The source and desolvation temperatures were 150 and 650°C, respectively. The collision energy of the MS–MS was between 10 and 50 eV. For the quantification of the molecules, we used three fragment ions, one for quantification and two for qualification. For internal standard calibration, two fragment ions were used. MS data were processed by using TargetLynx V4.1 SCN 904. The peak area of the diagnostic product ion was used for quantification. The limit of quantification was for CKs between 0.25 and 5, auxins 0.2 and 1.5, for ABA 2.5 and 5, for SA 3.5 and 7, ng g^{-1} sample DW.

2.9 | Statistical analysis

For comparison of parameters between the two lines, *CR2262* and *CR2267*, at individual timepoints, significance of differences was calculated by double-sided *t* test. One-way ANOVA with post hoc Tukey HSD testing was used for calculating the significance of B-dependent differences within a certain developmental stage (DAG) in a specific *B. napus* accession or for calculation of the significance of DAG-dependent differences within a certain B supply treatment within a specific accession.

3 | RESULTS

3.1 | Impact of the B supply on seedling growth, shoot biomass, and B accumulation in two *B. napus* accessions

The *B. napus* accessions *CR2267* (B-efficient) and *CR2262* (B-inefficient) (Pommerrenig, Junker, et al., 2018) were cultivated for 25 DAG on low (B-deficient), medium, or high soil B conditions. On medium or high B supply, both accessions reached the growth stages BBCH15-17 (five to seven leaves unfolded) (Meier, 2001) without significantly differing in their shoot biomass accumulation (Figures 1 and S1). Although shoot B concentrations and contents were significantly higher under high than under medium B supply at all time points in both accessions (except for 15 DAG when B concentrations did not significantly differ between medium and high B supply), the fresh and DWs of both accessions did not differ between these two treatments with the exception of *CR2267* at 5 DAG that exhibited a lower DW at high B when compared to medium B supply (Figure 1 and Tables S1 and S2). This indicated that the high B treatment provided excess B but did not induce B toxicity. Phenotypic differences between *CR2267* and *CR2262* on the B-deficient condition became visible at 6–8 DAG when the first true leaf appeared (Figure S1). The first leaf in *CR2267* developed and unfolded similarly to the medium B supply, while the one of *CR2262* arrested its growth under low B conditions (Figure S1). From 10 DAG, this was reflected in the significantly lower biomass accumulation of *CR2262* compared to *CR2267* (Figure 1A). Moreover, *CR2262* had a significant lower increase in DW than at the other B supply levels and displayed typical B-deficiency symptoms such as arrested shoot growth, malformed, cupped downward, and lanceolate new leaves, while cotyledons turned purple indicating an enhanced production of anthocyanins (Figure 1, Figure S1). During the first 15 days of growth, fresh and DWs of *CR2267* differed significantly between low and medium or high B but not between medium and high B supply. At the later stages, namely at 20 and 25 DAG, these differences became insignificant and plants grown on low, medium, and high B supply exhibited similar biomass. This was in stark contrast to *CR2262* where the biomass of plants grown under B deficiency was always lower when compared to plants grown on medium or high B supply conditions (Tables S1 and S2). This shows that in contrast to *CR2262*, *CR2267* had no growth retardation despite severe B-deficient growth conditions. Unexpectedly, apart from 10 DAG, the shoot B concentrations of *CR2267* did not differ significantly from the ones of *CR2262*, reaching only about 9 μg B (g^{-1} DW), a value five to ten times lower than that in leaves grown under medium or high B supply (Figure 1D) and clearly below the lower threshold of 15 μg B (g^{-1} DW) that is considered adequate for growth of oilseed rape (Bergmann, 1992; Dell & Huang, 1997; Husted et al., 2011). Under medium and high B supply, *CR2262* possessed higher B concentrations than *CR2267* (Figure 1), suggesting that transport pathways for B acquisition are effective in *CR2262*.

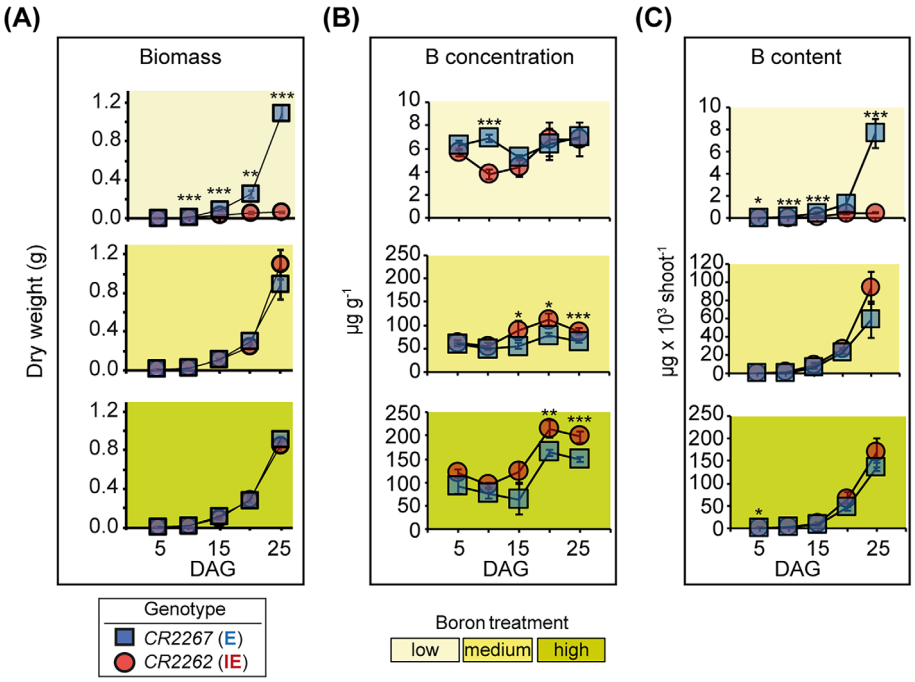

FIGURE 1 Biomass (A; left panel), boron concentrations (B; middle panel), and boron contents (C; right panel) of the *Brassica napus* accessions *CR2262* (B-inefficient; IE; red circles) and *CR2267* (B-efficient; E; blue squares). Plants were grown on low (light yellow; <0.1 mg B [kg soil]$^{-1}$), medium (beige; 2.4 mg B [kg soil]$^{-1}$) or high (khaki; 12.8 mg B [kg soil]$^{-1}$) B soil substrate concentrations and samples were taken 5, 10, 15, 20, and 25 days after germination (DAG). Symbols represent means and error bars display ±SE of four independently repeated trials, consisting of $n = 15–20$ (5 DAG), $n = 5–9$ (10 DAG), 5–7 (15 DAG), 3–5 (20 DAG), and 1–3 (25 DAG) plants. Asterisks indicate significant differences between IE and E, at the corresponding time point and growth condition (*$p < 0.05$, **$p < 0.01$, ***$p < 0.001$, *t* test)

3.2 | Impact of B supply on subcellular B partitioning in B-efficient and B-inefficient oilseed rape

The B requirement of plants is correlated with the amount of RG-II binding sites in the pectin fraction of cell walls (Hu & Brown, 1994; Matsunaga et al., 2004). We hypothesized that the vigorous growth of *CR2267* under low B supply compared to the B-inefficient *CR2262* accession is either due to a lower number of B-binding sites in the cell wall or due to its ability to efficiently locate the complete B pool to the pectic cell wall fraction where it is structurally needed. To address these possibilities, we conducted subcellular partitioning of B by discriminating water-soluble (cytoplasmic plus free apoplastic B fraction), acidic-extractable pectin (RG-II-containing fraction, from now on referred to as pectin fraction), and non-water-soluble (alkali-extractable pectin, hemicellulose, and cellulose fraction) fractions of *B. napus* shoots.

Under medium B conditions, averaged over all time points and both *B. napus* accessions, approximately 58% of the total B was detected in the water-soluble, approximately 41% in the pectin, and approximately 1% in the non-water-soluble fraction (Figure 2A). Under high B supply conditions, the surplus B was added to the water-soluble B (increase to approximately 70%) but not to the pectin (approximately 30%) or non-water-soluble (>1%) cell wall B fractions (Figure 2A). While the B concentration in the soluble B pool of both accessions markedly decreased from 30.7 ± 7.9 µg B g^{-1} DW in average at medium B supply to 1.8 ± 0.1 µg B g^{-1} DW in average at low B supply, the corresponding decrease was less pronounced in the pectin fraction, where B concentrations decreased only from 19.2 ± 3.3 to 7.4 ± 1.2 µg B (g^{-1} DW) in average, i.e., by approximately 61.5% compared to approximately 94.1% in the soluble B pool (Figure 2A). Under medium and high B supply growth conditions, *CR2262* exhibit higher shoot B concentrations compared to *CR2267* (Figure 1B). These higher shoot B concentrations result from a significantly higher B concentration in the soluble but not in the pectin bound or insoluble fractions (Figure 2). This suggests that the transport pathways for B acquisition and subcellular distributions are effective in *CR2262* and that the higher sensitivity of *CR2262* compared to *CR2267* toward B deprivation is unlikely to be explained by a generally higher *in muro* B demand of *CR2262*. Together, these analyses revealed that changes of the B supply levels caused significant fluctuations in the soluble B shares of the two accessions, while pectin-bound and non-water-soluble B fractions remained less affected (Figure 2A).

For comparison, we determined the cellular partitioning of Ca, which also takes part in cell wall-stabilizing functions of the pectic cell wall fraction. Additionally, it has been proposed that Ca partly complements cell wall defects caused by B deficiency. However, *CR2267* did not show significantly higher water-soluble or pectic Ca concentrations in the low versus medium and high B supply treatments, indicating that *CR2267* does not compensate for the lack of B by a surplus of Ca to stabilize cell walls (Figure 2B). In contrast, *CR2262* accumulated significantly more Ca in the pectin and water-soluble B fractions under low B supply when it suffered from B deficiency. This might either reflect a B-deficiency response mechanism of this accession to functionally compensate for the lack of B in its cell walls with an enhanced *in muro* inclusion of Ca or is the result of a continued Ca accumulation in a growth-retarded plant body.

3.3 | Boron-dependent accumulation of sugars and amino acids in B-efficient and B-inefficient oilseed rape

B deficiency-induced repression of photosynthesis is an often-observed phenomenon in many plant taxa (Cakmak & Römheld, 1997;

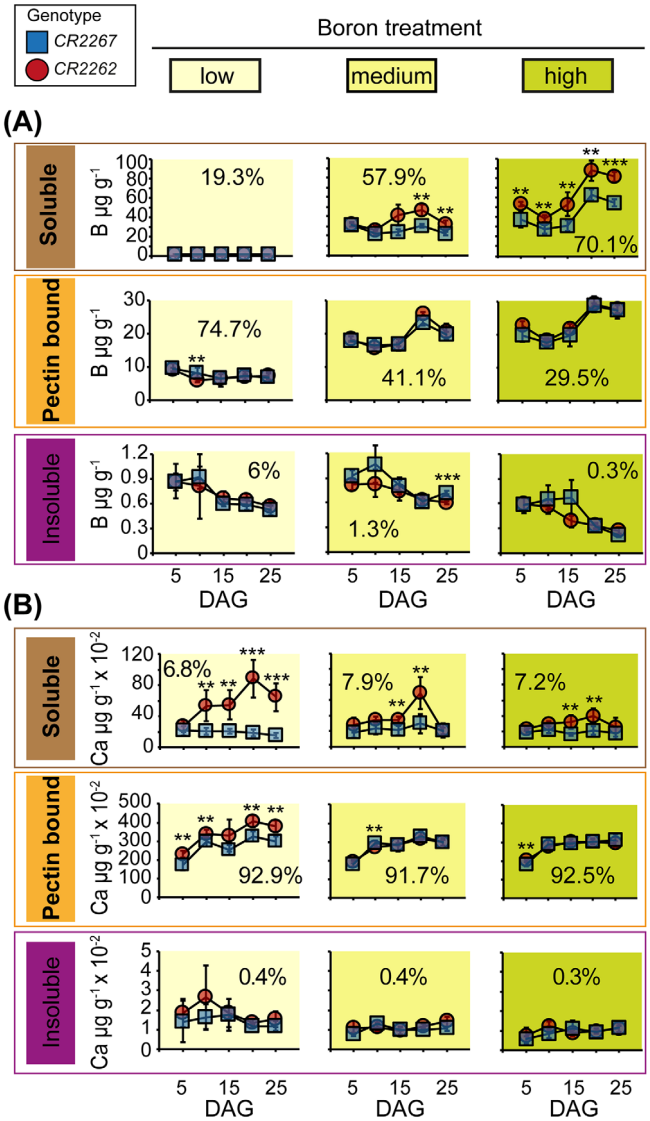

FIGURE 2 Subcellular shoot boron (B) and calcium (Ca) partitioning in a B-efficient and B-inefficient *Brassica napus* accession grown with different B supply levels. The *B. napus* accessions *CR2262* (B-inefficient; red circles) and *CR2267* (B-efficient; blue squares) were grown for 25 days on low (light yellow; <0.1 mg B [kg soil]$^{-1}$), medium (beige; 2.4 mg B [kg soil]$^{-1}$) or high (khaki; 12.8 mg B [kg soil]$^{-1}$) soil B concentrations. Samples were taken 5, 10, 15, 20, and 25 days after germination (DAG). Red and blue colored symbols represent means of B (A) or Ca (B) concentrations ± SE in µg per g dry weight of four independent biological repeated trials, consisting of $n = 15–20$ (5 DAG), $n = 5–9$ (10 DAG), 5–7 (15 DAG), 3–5 (20 DAG), and 1–3 (25 DAG) plants. Subcellular B and Ca concentrations were determined by ICP–MS analysis in the water-soluble (cytoplasmic plus free apoplastic B fraction; brown boxes), pectin-bound (the acid-extractable pectin RG-II-containing fraction; orange boxes) and the insoluble (non-water-soluble alkali-extractable pectin, hemicellulose, and cellulose fraction; purple boxes) fraction of *B. napus* shoots. The percentage value given per graph (rounded to the first decimal place) represents the share of B within the corresponding subcellular fraction from the measured total B content per shoot within the corresponding B supply condition averaged over both accessions and all time points. Asterisks indicate significant differences between *CR2262* and *CR2267* at the corresponding time point and growth condition (*$p < 0.05$, **$p < 0.01$, ***$p < 0.001$, double-sided Student's *t* test)

Marschner, 2012). At the same time, the accumulation of nonstructural carbohydrates such as sucrose is probably due to a decreased demand for growth and impaired vascular leaf efflux of reduced carbon out of source leaves into sinks (Camacho-Cristóbal & González-Fontes, 1999; Marschner, 2012). Such B deficiency-induced backlogging of soluble sugars causes even stronger feedback inhibition of photosynthesis, resulting in arrested growth and development. Therefore, the shoot sugar status can be seen as an indicator of the stress degree in plants facing B deficiency when compared to plants sufficiently supplied with B. At 5 DAG and under all B treatments, glucose and fructose accumulated at two to seven times higher concentrations in *CR2267* than in *CR2262*. Thereafter, glucose and fructose accumulated in a similar B- and developmental-dependent manner both in *CR2262* and *CR2267* (Figure 3). At later developmental stages, sucrose levels increased more strongly in *CR2262* over those in *CR2267* under low, but not under medium or high B conditions, indicating B deficiency-dependent impairment of vascular transport and backlog of carbon skeletons in *CR2262* leaves (Figure 3) coincided with the appearance of visible B-deficiency symptoms (Figure S1).

In the shoots of the B-efficient accession *CR2267*, alanine, leucine and the non-proteinogenic amino acid γ-aminobutyric acid (GABA) were the only amino acids that accumulated to a higher extent compared to *CR2262* during the B-deficient treatment. On the contrary, most of the other amino acids, most prominently the basic amino acids asparagine, arginine, histidine, and glutamine and the stress-related amino acid proline increased markedly in *CR2262* under low B supply conditions, indicating carbon and nitrogen overflow due to arrested growth and impaired leaf and cell elongation under B-limiting conditions (Figure S2). Together, these results indicate that B deficiency leads to an accumulation of primary C and N metabolites in *CR2262*, suggesting hampered downstream metabolism and conversion into macromolecules.

3.4 | Boron- and developmental-dependent changes in CK metabolism of B-efficient and B-inefficient oilseed rape

It was previously observed that CK levels drop drastically under limiting B supply during early seedling development of two B-inefficient oilseed rape cultivars (Eggert & von Wirén, 2017; Pommerrenig, Junker, et al., 2018). In Arabidopsis, the expression of the CK receptor gene *CRE1/WOL/AHK4*, which mediates CK signaling, is strongly inhibited under B-deficient conditions (Abreu et al., 2014). This indicates that plants require physiologically active CKs and subsequent signaling pathways to sustain growth. Therefore, we tested whether the levels of growth-promoting CKs differ between the B-efficient accession *CR2267* and the B-inefficient accession *CR2262*. In accordance with other studies, the active CK forms *trans*-zeatin (TZ), isopentenyladenine (IP), and *cis*-zeatin (CZ) were below the detection limit of 0.1 ng g^{-1} DW (Eggert & von Wirén, 2017; Tarkowska et al., 2012). Interestingly, the corresponding ribosylated forms IP-riboside (IPR), *cis*-zeatin-riboside (CZR) and *trans*-zeatin-riboside

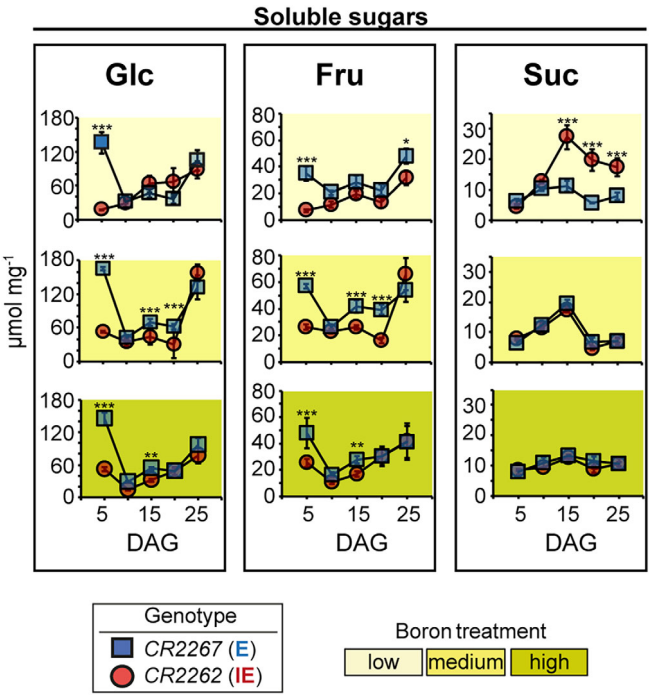

FIGURE 3 Quantifications of soluble sugars in shoots of two *Brassica napus* accessions contrasting in their boron (B) efficiency grown on three different soil B conditions. The concentration of glucose (Glc), fructose (Fru), and sucrose (Suc) was quantified in the shoots of the *B. napus* accessions *CR2262* (B-inefficient; red circles) and *CR2267* (B-efficient; blue squares). Plants were grown on low (light yellow; <0.1 mg B [kg soil]$^{-1}$), medium (beige; 2.4 mg B [kg soil]$^{-1}$) or high (khaki; 12.8 mg B [kg soil]$^{-1}$) B soil substrate concentrations and samples were taken 5, 10, 15, 20, and 25 days after germination (DAG). Red and blue colored symbols represent means of quantified sugar concentrations ±SE of four independent biological repeated trials, consisting of $n = 15–20$ (5 DAG), $n = 5–9$ (10 DAG), 5–7 (15 DAG), 3–5 (20 DAG), and 1–3 (25 DAG) plants. Asterisks indicate significant differences between *CR2262* and *CR2267*, at the corresponding time point and growth condition (**$p < 0.01$, ***$p < 0.001$, *t* test)

(TZR), which represent precursors and transport forms, accumulated to higher levels in *CR2267* compared to *CR2262* at 15, 20, and 25 DAG upon B-deficient condition (Figure 4). The accumulation of TZR was also inversely correlated with the B supply level at 20 and 25 DAG in *CR2267* but not *CR2262* (Table S1). In a developmental context, the accumulation of these CK species in *CR2267* coincided temporally with the outgrow of the shoot apical meristem and emergence of the first leaves after 10–15 DAG and was three to five times higher under low than under medium or high B supply. Under high B supply, IPR and CZR concentrations were lower in comparison to the medium B supply condition. A similar behavior of dihydro-zeatin riboside (DZR) was observed in *CR2262* only under B-limiting conditions (Figure 4). The concentration of the deactivated CK species *trans*-zeatin-O-glucoside (TZOG) was significantly higher in *CR2262* particularly under B-deficient conditions at all time points tested. The content of *cis*-zeatin-O-glucoside-riboside (CZROG) was significantly increased in *CR2262* compared to CR2267 at 15 DAG. However, no such increase was observed for the third inactive CK species, *trans*-zeatin-9-glucoside (TZ9G) (Figure 4). No such congruent pattern was observed for *CR2267*. TZOG concentrations were significantly higher in *CR2262* even during the complete time course under B-limiting conditions. Higher concentrations of inactive CK species were also observed occasionally in *CR2262* under medium and high B conditions. These results suggest that a decrease in B supply and shoot B concentrations may lead to an increase in the synthesis of CZ, TZ, DZ and IP via their immediate precursors in a developmentally- and genotype-dependent manner (Figure 4). In contrast, the inactive forms accumulated at much higher concentrations in *CR2262* than in *CR2267*, suggesting a role of active CK in the maintenance of the shoot meristem activity and proper leaf development of *CR2267* under low B conditions at the investigated developmental growth stages.

3.5 | Boron- and developmental-dependent changes in the auxin metabolism in B-efficient and B-inefficient oilseed rape

Besides CKs, auxins are crucial to regulating shoot apical meristem formation and functioning and subsequent organ growth (Schaller et al., 2015). To analyze the involvement of auxin in the accession-dependent response to different B supply levels, the concentration of indole-3-acetic acid (IAA) together with the auxin-precursor tryptophan, the biosynthetic intermediates indole-3-acetamide (IAM) and indole-3-acetonitrile (IAN), the reversible auxin storage forms IAA methyl ester (IAAMe), and indole-3-acetyl-L-alanine as well as the inactivated forms 2-oxindole-3-acetic acid, and IAA glutamic acid were measured in *CR2267* and *CR2262* (Figure 5). While the concentrations of the bioactive IAA species and its freely convertible storage form IAAMe were low at medium B conditions in *CR2262* and *CR2267*, they significantly increased by 16-fold in *CR2262* under B-deficient conditions. This result is in line with the strongly increased detected IAN concentration under low- compared to medium B supply. IAN has been reported to be the most abundant detectable precursor of IAA (Novak et al., 2012; Sugawara et al., 2009). In accordance with our expectation, a B deficiency-dependent increase of the conjugated auxin species IAA-Gluc was only detected in the B-inefficient but not the B-efficient accession (Figure 5, Table S1).

3.6 | Boron- and developmental-dependent changes in ABA metabolism in B-efficient and B-inefficient oilseed rape

The role of ABA is tightly connected to abiotic stress responses such as drought or nutrient deficiencies. The concentrations of the bioactive ABA itself, its storage and transport form, the glucosyl-ester (ABA-Glu), and the ABA catabolites phaseic acid (PA) and

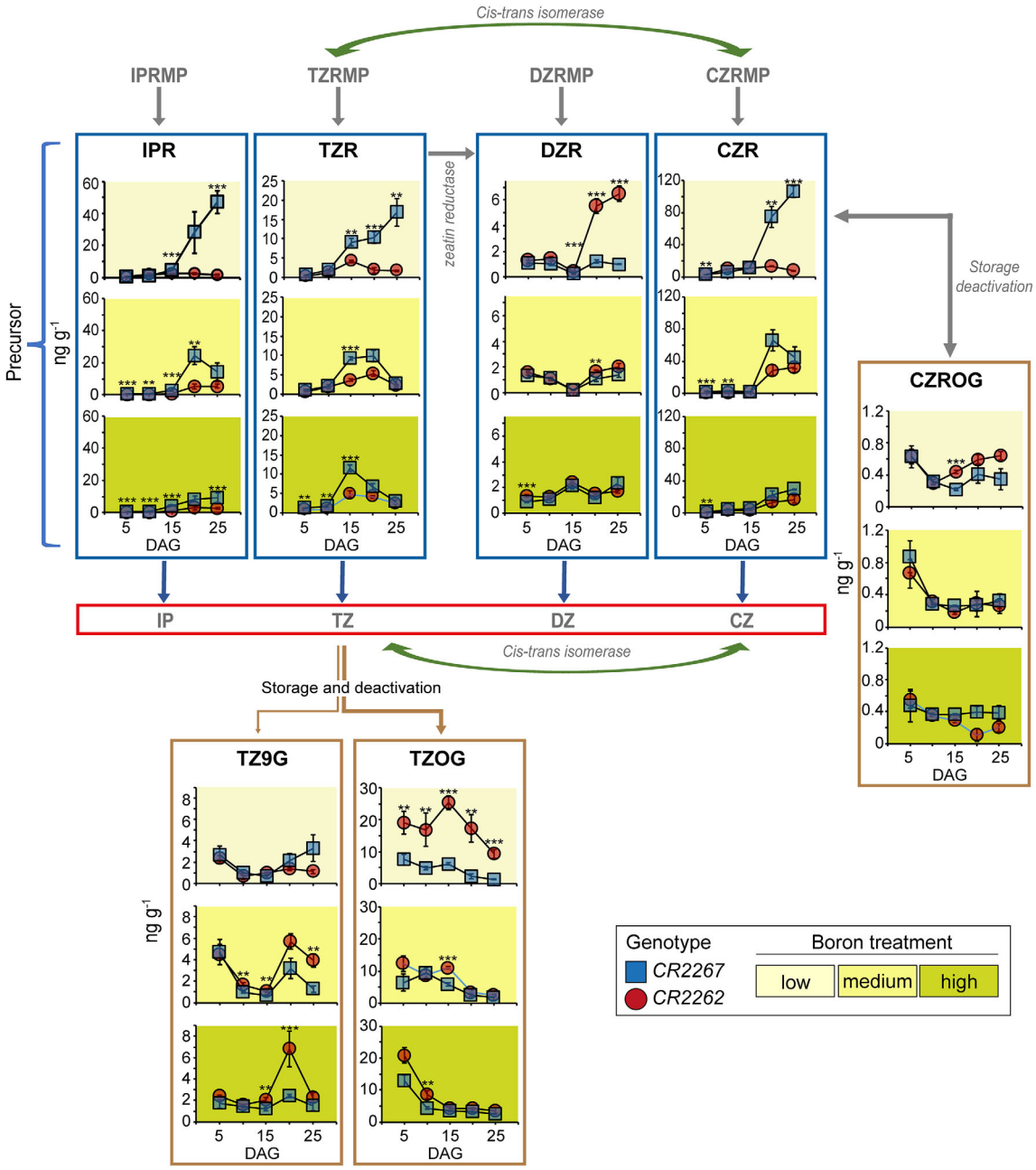

FIGURE 4 Cytokinin (CK) formation as a function of the developmental stage and the boron (B) supply regime in shoots of two *Brassica napus* accession contrasting in their B efficiency. The *B. napus* accession *CR2262* (B-inefficient; red circles) and *CR2267* (B-efficient; blue squares) contrasting in their B efficiency were grown for 25 days on low (light yellow; <0.1 mg B [kg soil]$^{-1}$), medium (beige; 2.4 mg B [kg soil]$^{-1}$) or high (khaki; 12.8 mg B [kg soil]$^{-1}$) B soil substrate concentrations and samples were taken 5, 10, 15, 20, and 25 days after germination (DAG). Red and blue colored symbols represent the means of concentrations of targeted CK metabolites ±SE in ng per g dry weight of four independent biological repeated trials, consisting of $n = 15–20$ (5 DAG), $n = 5–9$ (10 DAG), 5–7 (15 DAG), 3–5 (20 DAG), and 1–3 (25 DAG) plants. Colored arrows indicate the biosynthetic transformations of CK precursors and CKs in *B. napus*. Precursors (blue boxes), bioactive (red boxes), as well as storage and deactivated (brown boxes) forms are displayed. Non-detected and detected CK metabolites are written in gray and black colors, respectively. Enzymatic conversions of CK metabolites and underlying enzymes are displayed in dark green. Asterisks indicate significant differences between *CR2262* and *CR2267*, at the corresponding time point and growth condition (*$p < 0.05$, **$p < 0.01$, ***$p < 0.001$, double-sided Student's *t* test). CZ, cis-zeatin; CZR(MP), cis-zeatin-riboside (monophosphate); CZROG, cis-zeatin-*O*-glucoside riboside; DZ, dihydrozeatin; DZR(MP), dihydrozeatin-riboside (monophosphate); IPR (MP), N6-isopentenyladenosine (monophosphate); TZ, trans-zeatin IP, N6-isopentenyladenine; TZ9G, trans-zeatin N9-glucoside; TZOG, trans-zeatin-*O*-glucoside; TZR(MP), trans-zeatin-riboside (monophosphate)

dihydrophaseic acid (DHPA) were quantified (Figure 6). At 5 DAG, ABA concentrations in *CR2262* and *CR2267* were 1.9–3.8-fold or 1.5–2.2-fold higher under low B than under medium or high B supply conditions, respectively (Figure 6). At 10 DAG, *CR2262* had still significantly higher ABA levels under low compared to the medium B treatment (3.6-fold higher ABA levels). From 15 DAG on, ABA levels ranged mostly between 40 and 60 ng g^{-1} with little differences between the two accessions (Figure 6). While ABA-Glu levels remained below the detection level at 5 DAG, they increased from 10 DAG onward and reached eightfold higher values in *CR2262* than in *CR2267* under low B supply, they did not differ between these accessions in any of the other two B treatments. This strong genotype-dependent accumulation of ABA-Glu indicated B-deficiency and ABA-dependent responses in *CR2262* but not *CR2267* and confirmed the high free ABA levels of *CR2262* at the earlier timepoints (namely 5 and 10 DAG). PA and DHPA continuously increased independently of the B treatment and the genotype during the analyzed growth stages, which suggests a continuous ABA degradation with DHPA accumulating as the dominant species (Figure 6).

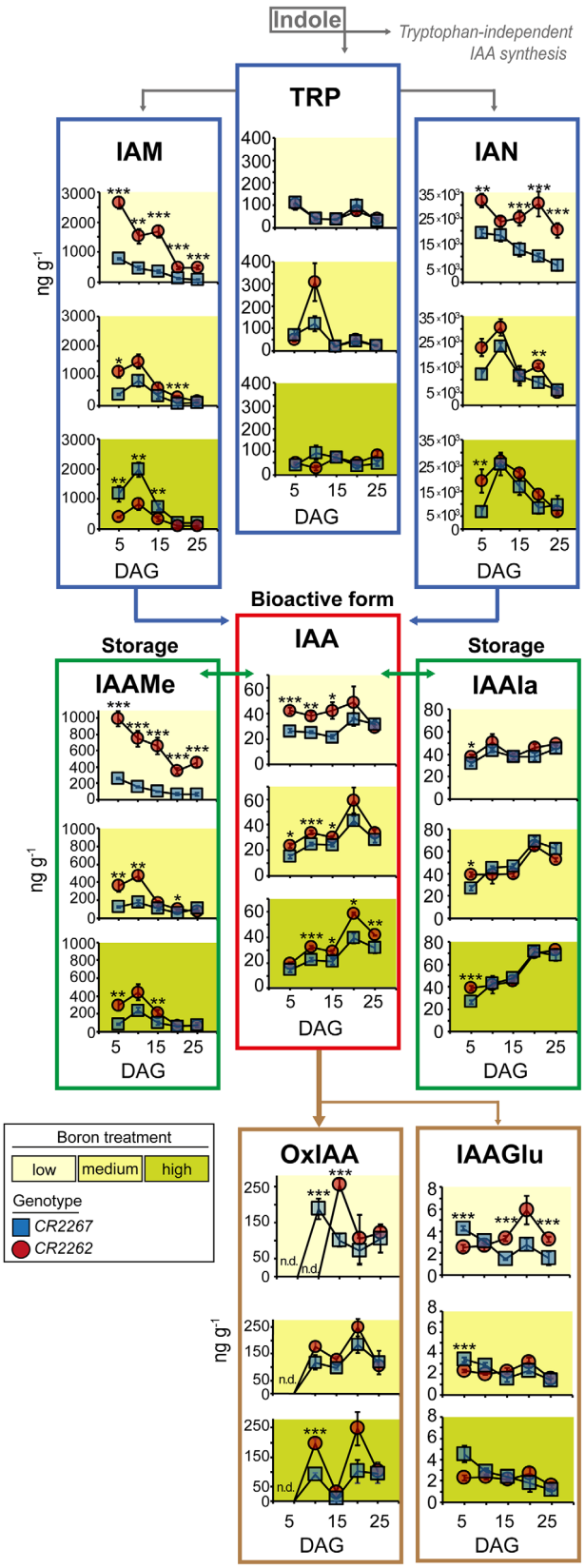

FIGURE 5 Auxin formation as a function of the developmental stage and the boron (B) supply regime in shoots of two *Brassica napus* accessions contrasting in their B efficiency. The *B. napus* accessions *CR2262* (B-inefficient; red circles) and *CR2267* (B-efficient; blue squares) contrasting in their B efficiency were grown for 25 days on low (light yellow; <0.1 mg B [kg soil]$^{-1}$), medium (beige; 2.4 mg B [kg soil]$^{-1}$) or high (khaki; 12.8 mg B [kg soil]$^{-1}$) B soil substrate concentrations and samples were taken 5, 10, 15, 20, and 25 days after germination (DAG). Red and blue colored symbols represent means of concentrations of targeted auxin metabolites ±SE in ng per g dry weight of four independent biological repeated trials, consisting of $n = 15–20$ (5 DAG), $n = 5–9$ (10 DAG), 5–7 (15 DAG), 3–5 (20 DAG), 1–3 (25 DAG) plants. "L-tryptophan" (TRP) indicates the starting point of TRP-dependent indole-3-acetic acid (IAA) biosynthesis. Gray arrows indicate the biosynthetic pathway of auxins in *B. napus*. Detected precursors (blue boxes), bioactive (red boxes), storage (green boxes), and inactivated (brown boxes) forms are displayed. Asterisks indicate significant differences between *CR2262* and *CR2267*, at the corresponding time point and growth condition (*$p < 0.05$, **$p < 0.01$, ***$p < 0.001$, double-sided Student's *t* test). IAAGlu, indole-3-acetyl-L-glutamic acid; IAAIa, indole-3-acetyl-L-alanine; IAAMe, indole-3-acetic acid methyl ester; IAM, indole-3-acetamide; IAN, indole-3-acetonitrile; OxIAA, 2-oxoindole-3-acetic acid

3.7 | Boron- and developmental-dependent changes in salicylic acid (SA) metabolism in B-efficient and B-inefficient oilseed rape

SA levels are mainly associated with the response of plants to biotic and abiotic stress. In contrast to such proposed functions, the SA levels did not differ between the two accessions under B deficiency with the exception of 10 DAG where SA levels were significantly higher in *CR2267* compared to *CR2262*. They were, however, hardly influenced by the B supply level in either of the two accessions (Figure S3, Table S2). From 5 DAG, SA levels strongly decreased to a

similar extent in both accessions and independent of the B treatment (Figure S3). Together, our results suggest that B deficiency does not represent an abiotic stress factor significantly increasing SA concentrations in neither *CR2267* nor *CR2262*.

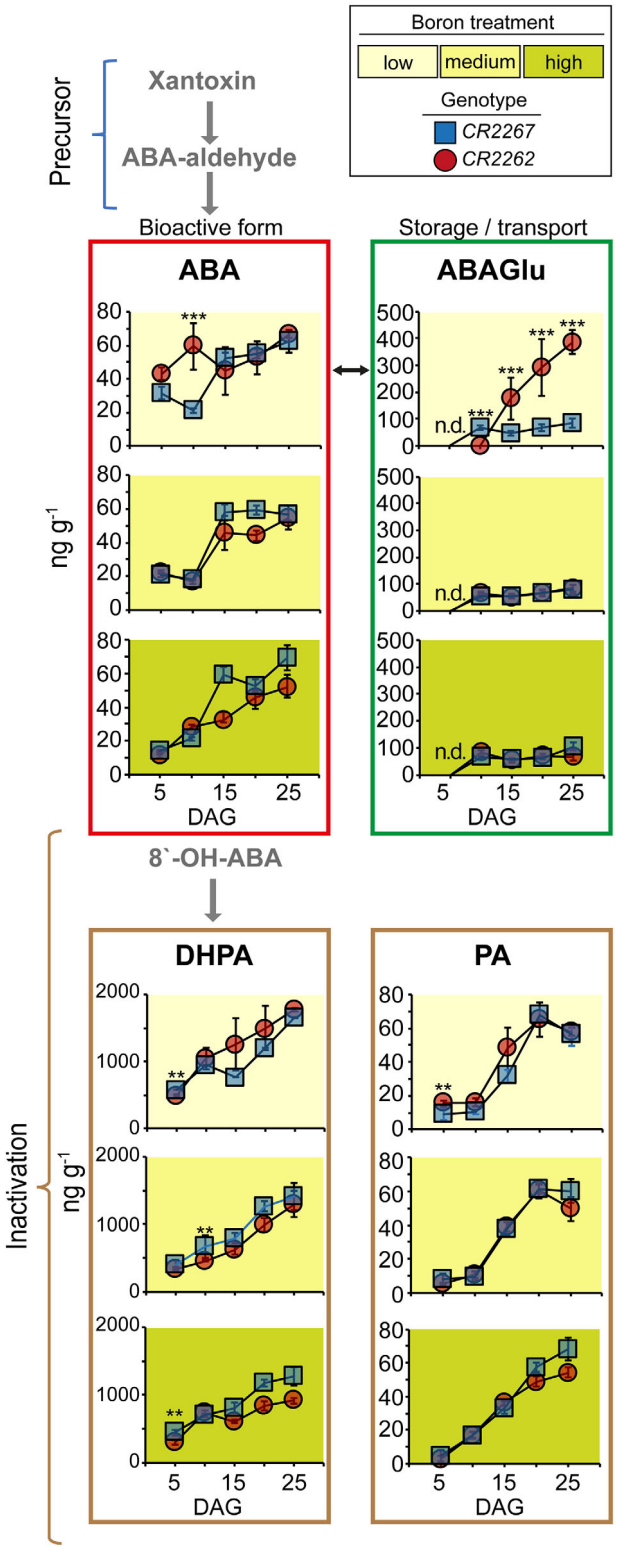

4 | DISCUSSION

4.1 | Under B-sufficient conditions, the majority of B is soluble and not bound to the cell walls of oilseed-rape

Our results regarding the B partitioning between "soluble" (i.e., B not associated with the cell wall) and "insoluble" (i.e., B associated with the cell wall) cellular fractions are in accordance with previous reports, namely that the majority of B is soluble and not bound to the cell wall under B-sufficient conditions (Hu & Brown, 1994; Matoh & Ochiai, 2005; Matsunaga et al., 2004). This fact is largely disregarded in the literature, where it is mostly stated that most of the B is found in cell walls. According to our results and that of others (Hu & Brown, 1994; Matoh & Ochiai, 2005; Matsunaga et al., 2004), this is only true under B-deficient conditions in which the amount of "soluble" B declines dramatically while the "insoluble" proportion of cellular B increases.

4.2 | Boron efficiency in *CR2267* does neither depend on B accumulation nor on subcellular B partitioning

Nutrient efficiencies are frequently associated with the ability of a genotype to efficiently acquire the corresponding nutrient from the growth substrate. Here, the B-efficient growth of the *B. napus* accession *CR2267* in comparison to *CR2262* is shown to be caused by plant traits independent of the B-uptake capacity. As reported earlier, the growth of *CR2267* and *CR2262* differed significantly under B deficiency but not under sufficient B supply (Pommerrenig, Junker, et al., 2018). Here, we show that, under limiting B supply, *CR2267* had similar growth and leaf development as under higher B supplies,

FIGURE 6 Formation of the phytohormone abscisic acid (ABA) as well as its storage/transport and inactivated forms as a function of the developmental stage and the boron (B) supply regime in shoots of two *Brassica napus* accessions contrasting in their B efficiency. The *B. napus* accession *CR2262* (B-inefficient; red circles) and *CR2267* (B-efficient; blue squares) contrasting in their B efficiency were grown for 25 days on low (light yellow; <0.1 mg B [kg soil]$^{-1}$), medium (beige; 2.4 mg B [kg soil]$^{-1}$) or high (khaki; 12.8 mg B [kg soil]$^{-1}$) B soil substrate concentrations and samples were taken 5, 10, 15, 20, and 25 days after germination (DAG). Red and blue colored symbols represent means of concentrations of targeted molecules of the ABA metabolism ±SE in ng per g dry weight of four independent biological repeated trials, consisting of $n = 15–20$ (5 DAG), $n = 5–9$ (10 DAG), 5–7 (15 DAG), 3–5 (20 DAG), and 1–3 (25 DAG) plants. Asterisks indicate significant differences between *CR2262* and *CR2267*, at the corresponding time point and growth condition (***$p < 0.001$, double-sided Student's *t* test). Xantoxin and ABA-aldehyde represent precursors of the bioactive ABA form. ABA-Glu (glucosyl-ester of ABA) represents the storage form of ABA. 8′-hydroxy ABA (8′-OH-ABA), dihydrophaseic acid (DHPA), and phaseic acid (PA) represent the catabolic inactivation products of ABA. (n.d., not detectable)

characterizing *CR2267* as highly tolerant to B deficiency (Figures 1 and S1). Interestingly, B shoot concentrations of *CR2267* under limiting B supply were clearly below 15 μg B (g^{-1} DW), a critical threshold for adequate growth of oilseed rape (Bergmann, 1992; Dell & Huang, 1997; Husted et al., 2011). A simple explanation may be that *CR2267* has a low demand for B. This may be the case if its primary cell wall, the only known cellular compartment in which B has a structural function, has a lower B-binding capacity when compared to B-inefficient accessions. However, we could not confirm this hypothesis, as we found similar and not significantly different amounts of B in the pectic cell wall fraction of *CR2267* at any developmental stage or B supply level (Figure 2). This indicates that the pectin fraction of the primary cell wall is a B sink of similar strength in *CR2267* and *CR2262* and indicates that the efficient accession *CR2267* does not require less B to cover the B demand of its pectin fraction. Consistently, in the low B treatment, neither leaf B concentrations nor subcellular B partitioning differed between *CR2267* and *CR2262*. *CR2267* showed no growth retardation with a pectin B concentration at which the leaf development in *CR2262* was completely suppressed. It is unlikely that the potential B binding sites in the pectin layer of *CR2262* were insufficiently occupied under low B supply, since B concentrations of this fraction increased only marginally with increasing B supply and higher B contents and concentrations in *CR2262* under medium and high B supply caused B accumulation exclusively in the water-soluble, but not in the pectin fraction. These results indicated that the pectin fraction is able to absorb most of the available B even under very limiting B supply. Furthermore, the results suggested that (1) growth reduction of *CR2262* plants did rather coincide with a drastic decline in the soluble B share unrelated to primary cell wall metabolism, (2) the continuous growth of *CR2267* under B limitations was not caused by a higher share of *in muro* located Ca that may compensate biochemically for the lack of B, and (3) the accession *CR2267* has a higher B utilization efficiency, by which even little B quantities suffice to maintain developmental and metabolic processes.

4.3 | B deficiency impairs primary metabolism in B-inefficient oilseed rape

Accumulation of the monosaccharides glucose and fructose and the disaccharide sucrose in plant tissues is a frequently observed consequence of abiotic stresses (Hanson & Smeekens, 2009; Ohto et al., 2001; Pommerrenig, Ludewig, et al., 2018). The physiological effects provoked by sugar accumulation differ depending on the stress state of the sugar-accumulating tissue (Granot et al., 2014; Ruan, 2014; Wingler & Roitsch, 2008). High monosaccharide concentrations in rapidly growing young tissues, as present in the seedlings and plants analyzed here, can promote cell proliferation and the outgrowth of new leaves (Skylar et al., 2011). Under unfavorable conditions or arrested growth, however, sucrose utilization in sinks is reduced and sucrose may backlog in the phloem resulting in sucrose overflow in the cytosol and possible detrimental effects (Ruan, 2014). Such a situation was likely to occur here in *CR2262* plants under low B. Under the different B conditions tested here, sucrose accumulated at significantly higher concentrations in *CR2262* under low B, indicating that sucrose transport via the phloem into sinks was impaired in *CR2262* (Figure 3). In *CR2267*, which did not arrest growth under low B, sucrose was apparently efficiently transported and metabolized to sustain growth and biomass accumulation, indicating functional vascular transport and downstream metabolism even under limiting B supply.

Most free amino acids over-accumulated in *CR2262* during B-deficient conditions (Figure S2). Especially N-rich amino acids like glutamine, asparagine, lysine, histidine, and arginine accumulated in large amounts in *CR2262*, indicating that these amino acids accumulated in consequence of the hampered downstream conversion of amino nitrogen. Also, amino acids serine, tyrosine, valine, and stress-related proline, accumulated to high levels in *CR2262* under low B, but not in *CR2267* (Figure S2). This indicated that free amino acids were not used for biomass production but rather represented impaired sink activity and protein biosynthesis. Notably, the non-proteinogenic amino acid GABA accumulated to higher concentrations in *CR2267* in comparison to *CR2262* under low B. GABA accumulation is provoked by abiotic stresses like salt, cold, and drought, and inhibits cell elongation (but not division) in a dose-dependent manner (Baum et al., 1996; Häusler et al., 2014; Kinnersley & Turano, 2000; Ramesh et al., 2017). It may therefore be possible that the B-dependent accumulation of GABA in *CR2267* contributes to the regulation of cell elongation in combination with other signaling compounds under low B conditions.

4.4 | Roles of auxin and ABA in differential B efficiency

Elevated levels of bioactive auxins have been speculated to cause growth-retarding effects in shoots of B-inefficient *B. napus* accessions grown under B-deficient growth conditions (Eggert & von Wirén, 2017; Zhou et al., 2016). In our experiments, concentrations of the physiologically most active auxin species, IAA, showed rather a higher dependence on the developmental stage than on B supply levels (Figure 5). Nevertheless, IAA levels of the B-inefficient accession *CR2262* significantly increased under B-deficient conditions in contrast to the B-efficient accession *CR2267* (Figure 5). Considering that auxin may counteract the growth-promoting effect of CKs in leaves (Schaller et al., 2015), higher IAA and lower CK levels in *CR2262* compared to *CR2267*, may have contributed to growth suppression of *CR2262* via an unfavorable CK versus auxin balance. In general, the dynamic pattern of several auxin derivatives in *CR2267* appeared independent of its B nutritional status, indicating that auxin metabolism made a minor contribution to its superior B-deficiency tolerance matching previous observations (Zhou et al., 2016). Together, these results suggest that auxins were not substantially involved in the B deficiency response itself but rather via its interaction with CK levels.

ABA is a stress-related signaling molecule known to function in response to nutrient deficiencies such as Mg, S, P, and N (Hermans

et al., 2010; Koprivova & Kopriva, 2016; Oka et al., 2012; Woo et al., 2012). Also, B-deprived *B. napus* plants accumulate more ABA than plants growing under B-sufficient conditions (Eggert & von Wirén, 2017; Zhou et al., 2016). Zhou et al. (2016) observed a drastically increased shoot ABA concentration after 3–5 days of B deficiency in a B-inefficient but not a B-efficient accession. Alike, we observed a significant ABA peak in *CR2262* but not in *CR2267* around 10 DAG. This suggests that transiently elevated shoot ABA levels are common to B deficiency-sensitive accessions in which ABA might induce the expression of B channels being of crucial importance for B nutrition (Gómez-Soto et al., 2019). Respecting the timely increase in ABA levels in *CR2262* already at 10 DAG, ABA can be classified as an early B deficiency response preceding the subsequent growth retardation.

4.5 | CKs as early B deficiency signals in B-efficient oilseed rape

Previous studies in oilseed rape and Arabidopsis have reported that shoot CK levels correlate positively with shoot B concentrations and plant growth, supporting their importance as early signaling compounds under low-B stress (Eggert & von Wirén, 2017; Poza-Viejo et al., 2018). While those studies were conducted with B-inefficient accessions, we tested the hypothesis whether shoot CK levels also associate with B efficiency. Indeed, in contrast to *CR2262*, the B-efficient accession *CR2267* showed strongly B-dependent accumulation of the ribosylated CK species IPR, CZR, and TZR (Figure 4). Importantly, the significant accumulation of these CK species in *CR2267* coincided with the emergence of the first vegetative leaves at 10–15 DAG (Figure 4), which defines a period of rapid growth rates, and thus of high B demand, which depends on a properly functioning shoot apical meristem. Most strikingly, the concentrations of these CK species were three to five times higher under low than under medium or high B supply conditions, emphasizing their importance as shoot growth-promoting signals, especially under low-B conditions. In support of this function, we recently reported a strong accumulation of IPR, CZR, and TZR under B-deficient conditions in common plantain (*Plantago major* L.), a species with high tolerance against B deficiency during vegetative growth (Pommerrenig et al., 2019). Respecting the lack of increase of deactivated CK species in the B-efficient accession (Figure 4), the increase in ribosylated CK species, which are the immediate precursors for the physiologically active, de-ribosylated species (Kudo et al., 2010), indicates that these CK pools were fueled by de-novo synthesis. The fact that IPR, TZR and CZR concentrations increased in *CR2267* with decreasing B nutritional status while shoot biomass remained constant (Figure 1) allows us to speculate that the abundance of these CKs was not a consequence of better plant growth but a B-deficiency response that most likely caused better plant growth. In Arabidopsis, a biochemical study investigating the hormone-binding characteristics of AHK3, the CK receptor playing a predominant role in shoot development, demonstrated that TZ and TZR possess a much stronger binding capacity than DZ (Romanov et al., 2006). This might explain why the accumulation of TZR, CZR, and IPR observed exclusively in the B-efficient accession sustains shoot apical meristem activity and leaf growth under low-B conditions. In contrast, the quantitatively minor accumulation of the weakly active CK species DZR in *CR2262* failed to do so (Figure 4). The fact that the CK forms with a high affinity to shoot CK receptors accumulated exclusively in the B-efficient accession, while the less active form DZR and the deactivated species CZROG and TZOG accumulated in the B-inefficient accession, points to a shoot growth-regulating role of these CK species, especially under low B. This conclusion is in line with the recent finding that CK signaling regulates early responses of B deficiency in maize, where a B-dependent CK signaling was shown to be important to prevent the progressive impairment of meristem development revealed by vegetative and reproductive defects (Matthes et al., 2022). Moreover, overexpression of a CK oxidase in maize roots, which leads to reduced CK levels, was shown to influence the shoot content of various nutrients (Ramireddy et al., 2021). This suggests that CK levels might be instrumental for the acclimatization of plants to various nutrient stresses. We thus conclude that *CR2267* translates B deficiency into CK biosynthesis to sustain vigorous growth.

AUTHOR CONTRIBUTIONS

Benjamin Pommerrenig and Gerd Patrick Bienert conceived the study and wrote the paper together with Nicolaus von Wirén. Benjamin Pommerrenig and Maximilian Faber conducted most of the experiments. Mohammad-Reza Hajirezaei performed carbohydrate and amino acid analyses. Benjamin Pommerrenig, Gerd Patrick Bienert, Mohammad-Reza Hajirezaei, and Nicolaus von Wirén analyzed the data.

ACKNOWLEDGMENTS

The authors dedicate this work to the memory of their friend and colleague, Dr Kai Eggert without whose consolidated knowledge and exceptional analytic skill set on plant hormones this study would not have been successful. Unfortunately, Kai Eggert passed away on August 13, 2018. The authors would also like to thank Jacqueline Fuge, Annett Bieber, Felix Kuemmerer, and Nicole Schäfer (IPK-Gatersleben, Germany) for excellent technical assistance and Dr Yudelsy Tandron Moja (IPK-Gatersleben, Germany) for ICP–MS analyses. This work was supported by the Emmy Noether grant 1668/1-1 and 1668/1-2 from the Deutsche Forschungsgemeinschaft (to G.P.B.). Open Access funding enabled and organized by Projekt DEAL.

CONFLICT OF INTEREST

The authors declare no conflict of interest.

DATA AVAILABILITY STATEMENT

The author responsible for distribution of materials integral to the findings presented in this article in accordance with the policy described in the author guidelines is Gerd Patrick Bienert (patrick.bienert@tum.de).

ORCID

Benjamin Pommerrenig https://orcid.org/0000-0002-7522-7942
Mohammad-Reza Hajirezaei https://orcid.org/0000-0002-9537-0121
Nicolaus von Wirén https://orcid.org/0000-0002-4966-425X
Gerd Patrick Bienert https://orcid.org/0000-0001-9345-4666

REFERENCES

Abreu, I., Poza, L., Bonilla, I. & Bolaños, L. (2014) Boron deficiency results in early repression of a cytokinin receptor gene and abnormal cell differentiation in the apical root meristem of *Arabidopsis thaliana*. *Plant Physiology and Biochemistry*, 77, 117–121. https://doi.org/10.1016/j.plaphy.2014.02.008

Baum, G., Lev-Yadun, S., Fridmann, Y., Arazi, T., Katsnelson, H., Zik, M. et al. (1996) Calmodulin binding to glutamate decarboxylase is required for regulation of glutamate and GABA metabolism and normal development in plants. *The EMBO Journal*, 15, 2988–2996.

Bergmann, W. (1992) *Nutritional disorders of plants*. Jena: Gustav Fischer Verlag.

Cakmak, I. & Römheld, V. (1997) Boron deficiency-induced impairments of cellular functions in plants. *Plant and Soil*, 193, 71–83.

Camacho-Cristóbal, J.J. & González-Fontes, A. (1999) Boron deficiency causes a drastic decrease in nitrate content and nitrate reductase activity, and increases the content of carbohydrates in leaves from tobacco plants. *Planta*, 209, 528–536.

Dell, B. & Huang, L.B. (1997) Physiological response of plants to low boron. *Plant and Soil*, 193, 103–120.

Eggert, K. & von Wirén, N. (2013) Dynamics and partitioning of the ionome in seeds and germinating seedlings of winter oilseed rape. *Metallomics*, 5, 1316–1325. https://doi.org/10.1039/c3mt00109a

Eggert, K. & von Wirén, N. (2015) The role of boron nutrition in seed vigour of oilseed rape (*Brassica napus L.*). *Plant and Soil*, 402, 63–76. https://doi.org/10.1007/s11104-015-2765-1

Eggert, K. & von Wirén, N. (2017) Response of the plant hormone network to boron deficiency. *New Phytologist*, 216, 868–881. https://doi.org/10.1111/nph.14731

Fleischer, A., O'Neill, R. & Ehrwald, R. (1999) The pore size of non-graminaceous plant cell walls is rapidly decreased by borate ester cross-linking of the pectic polysaccharide rhamnogalacturonan II. *Plant Physiology*, 121, 829–838.

Goldbach, H.E., Yu, Q., Wingender, R., Schulz, M., Wimmer, M., Findeklee, P. et al. (2001) Rapid response reactions of roots to boron depriviation. *Journal of Soil Science and Plant Nutrition*, 164, 173–181.

Gómez-Soto, D., Galván, S., Rosales, E., Bienert, P., Abreu, I., Bonilla, I. et al. (2019) Insights into the role of phytohormones regulating pAtNIP5;1 activity and boron transport in *Arabidopsis thaliana*. *Plant Science*, 287, 110198. https://doi.org/10.1016/j.plantsci.2019.110198

Granot, D., Kelly, G., Stein, O. & David-Schwartz, R. (2014) Substantial roles of hexokinase and fruktokinase in the effects of sugars on plant physiology and development. *Journal of Experimental Botany*, 65, 809–819. https://doi.org/10.1093/jxb/ert400

Gupta, U.C. (1980) Boron nutrition of crops. *Advances in Agronomy*, 31, 273–307. https://doi.org/10.1016/S0065-2113(08)60142-X

Hajirezaei, M.R., Takahata, Y., Trethewey, R.N., Willmitzer, L. & Sonnewald, U. (2000) Impact of elevated cytosolic and apoplastic invertase activity on carbon metabolism during potato tuber development. *Journal of Experimental Botany*, 51, 439–445.

Hanson, J. & Smeekens, S. (2009) Sugar perception and signaling—an update. *Current Opinion in Plant Biology*, 12, 562–567.

Häusler, R.E., Ludewig, F. & Krueger, S. (2014) Amino acids—a life between metabolism and signalling. *Plant Science*, 229, 225–237.

Hermans, C., Vuylsteke, M., Coppens, F., Craciun, A., Inzé, D. & Verbruggen, N. (2010) Early transcriptomic changes induced by magnesium deficiency in *Arabidopsis thaliana* reveal the alteration of circadian clock gene expression in roots and the triggering of abscisic acid-responsive genes. *New Phytologist*, 187, 119–131. https://doi.org/10.1111/j.1469-8137.2010.03258.x

Hu, H. & Brown, P.H. (1994) Localization of boron in cell walls of squash and tobacco and its association with pectin (evidence for a structural role of boron in the cell wall). *Plant Physiology*, 105, 681–689.

Husted, S., Persson, D.P., Laursen, K.H., Hansen, T.H., Pedas, P., Schiller, M. et al. (2011) Review: the role of atomic spectrometry in plant science. *The Journal of Analytical Atomic Spectrometry*, 26, 52–79. https://doi.org/10.1039/C0JA00058B

Jia, Z., Giehl, R.F.H., Meyer, R.C., Altmann, T. & von Wirén, N. (2019) Natural variation of BSK3 tunes brassinosteroid signaling to regulate root foraging under low nitrogen. *Nature Communications*, 10, 2378. https://doi.org/10.1038/s41467-019-10331-9

Kinnersley, A.M. & Turano, F.J. (2000) Gamma aminobutyric acid (GABA) and plant responses to stress. *Critical Reviews in Plant Sciences*, 19, 479–509. https://doi.org/10.1080/07352680091139277

Kobayashi, M., Matoh, T. & Azuma, J. (1996) Two chains of rhamnogalacturonan II are cross-linked by borate-diol ester bonds in higher plant cell walls. *Plant Physiology*, 110, 1017–1020.

Koprivova, A. & Kopriva, S. (2016) Hormonal control of sulfate uptake and assimilation. *Plant Molecular Biology*, 91, 617–627. https://doi.org/10.1007/s11103-016-0438-y

Kudo, T., Kiba, T. & Sakakibara, H. (2010) Metabolism and long-distance translocation of cytokinins. *Journal of Integrative Plant Biology*, 52, 53–60. https://doi.org/10.1111/j.1744-7909.2010.00898.x

Lewis, D.H. (2019) Boron: the essential element for vascular plants that never was. *New Phytologist*, 221, 1685–1690. https://doi.org/10.1111/nph.15519

Marschner, H. (2012) *Marschner's mineral nutrition of higher plants*. London: Academic Press.

Matoh, T. & Ochiai, K. (2005) Distribution and partitioning of newly taken-up boron in sunflower. *Plant and Soil*, 278, 351–360.

Matsunaga, T., Ishii, T., Matsumoto, S., Higuchi, M., Darvill, A., Albersheim, P. et al. (2004) Occurence of primary cell wall polysaccharide rhamnogalacturonan II in pteridophytes, lycophytes, and bryophytes. Implications for the evolution of vascular plants. *Plant Physiology*, 134, 339–351.

Matthes, M.S., Darnell, Z., Best, N.B., Guthrie, K., Robil, J.M., Amstutz, J. et al. (2022) Defects in meristem maintenance, cell division, and cytokinin signaling are early responses in the boron deficient maize mutant tassel-less1. *Physiologia Plantarum*, 174, e13670.

Meier, U. (2001) *Growth stages of mono- and dicotyledonous plants*. Berlin, Germany: German Federal Biological Research Centre for Agriculture and Forestry, BBCH-Monograph, Blackwell Science.

Novak, O., Henykova, E., Sairanen, I., Kowalczyk, M., Pospisil, T. & Ljung, K. (2012) Tissue-specific profiling of the *Arabidopsis thaliana* auxin metabolome. *Plant Journal*, 72, 523–536.

Ohto, M.-A., Onai, K., Furukawa, Y., Aoki, E., Araki, T. & Nakamura, K. (2001) Effects of sugar on vegetative development and floral transition in Arabidopsis. *Plant Physiology*, 127, 252–261.

Oka, M., Shimoda, Y., Sato, N., Inoue, J., Yamazaki, T., Shimomura, N. et al. (2012) Abscisic acid substantially inhibits senescence of cucumber plants (*Cucumis sativus*) grown under low nitrogen conditions. *Journal of Plant Physiology*, 169, 789–796. https://doi.org/10.1016/j.jplph.2012.02.001

O'Neill, M.A., Ishii, T., Albersheim, P. & Darvill, A.G. (2004) Rhamnogalacturonan II: structure and function of a borate cross-linked cell wall pectic polysaccharide. *Annual Review of Plant Biology*, 55, 109–139.

Pommerrenig, B., Eggert, K. & Bienert, G.P. (2019) Boron deficiency effects on sugar, ionome, and phytohormone profiles of vascular and non-vascular leaf tissues of common plantain (*Plantago major L.*). *International Journal of Molecular Sciences*, 20, 3882.

Pommerrenig, B., Junker, A., Abreu, I., Bieber, A., Fuge, J., Willner, E. et al. (2018) Identification of rapeseed (*Brassica napus*) cultivars with a high tolerance to boron-deficient conditions. *Frontiers in Plant Science*, 9, 1142. https://doi.org/10.3389/fpls.2018.01142

Pommerrenig, B., Ludewig, F., Cvetkovic, J., Trentmann, O., Klemens, P.A. W. & Neuhaus, H.E. (2018) In concert: orchestrated changes in carbohydrate homeostasis are critical for plant abiotic stress tolerance. *Plant and Cell Physiology*, 59, 1290–1299.

Poza-Viejo, L., Abreu, I., González-García, M.P., Allauca, P., Bonilla, I., Bolaños, L. et al. (2018) Boron deficiency inhibits root growth by controlling meristem activity under cytokinin regulation. *Plant Science*, 270, 176–189. https://doi.org/10.1016/j.plantsci.2018.02.005

Ramesh, S.A., Tyerman, S.D., Gilliham, M. & Xu, B. (2017) γ-Aminobutyric acid (GABA) signalling in plants. *Cellular and Molecular Life Sciences*, 74, 1577–1603.

Ramireddy, E., Nelissen, H., Leuendorf, J.E., Van Lijsebettens, M., Inzé, D. & Schmülling, T. (2021) Root engineering in maize by increasing cytokinin degradation causes enhanced root growth and leaf mineral enrichment. *Plant Molecular Biology*, 106, 555–567. https://doi.org/10.1007/s11103-021-01173-5

Romanov, G.A., Lomin, S.N. & Schmülling, T. (2006) Biochemical characteristics and ligand-binding properties of Arabidopsis cytokinin receptor AHK3 compared to CRE1/AHK4 as revealed by a direct binding assay. *Journal of Experimental Botany*, 57, 4051–4058. https://doi, https://doi.org/10.1093/jxb/erl179

Ruan, Y.-L. (2014) Sucrose metabolism: gateway to diverse carbon use and sugar signaling. *Annual Review of Plant Biology*, 65, 33–67.

Rubio, V., Bustos, R., Irigoyen, M.L., Cardona-Lopez, X., Rojas-Triana, M. & Paz-Ares, J. (2009) Plant hormones and nutrient signaling. *Molecular Biology*, 69, 361–373. https://doi.org/10.1007/s11103-008-9380-y

Ryden, P., Sugimoto-Shirasu, K., Smith, A.C., Findlay, K., Reiter, W.D. & McCann, M.C. (2003) Tensile properties of Arabidopsis cell walls depend on both a xyloglucan cross-linked microfibrillar network and rhamnogalacturonan II-borate complexes. *Plant Physiology*, 132, 1033–1040.

Schaller, G.E., Bishopp, A. & Kieber, J.J. (2015) The yin-yang of hormones: cytokinin and auxin interactions in plant development. *The Plant Cell*, 27, 44–63.

Skylar, A., Sung, A., Hong, F., Chory, J. & Wu, X. (2011) Metabolic sugar signal promotes *Arabidopsis* meristematic proliferation via G2. *Developmental Biology*, 351, 82–89.

Sugawara, S., Hishiyama, S., Jikumaru, Y., Hanada, A., Nishimura, T., Koshiba, T. et al. (2009) Biochemical analyses of indole-3-acetaldoximedependent auxin biosynthesis in Arabidopsis. *Proceedings of the National Academy of Sciences of the United States of America*, 106, 5430–5435.

Sultan, S.E. (2000) Phenotypic plasticity for plant development, function and life history. *Trends in Plant Science*, 5, 537–542.

Takano, J., Wada, M., Ludewig, U., Schaaf, G., von Wirén, N. & Fujiwara, T. (2006) The Arabidopsis major intrinsic protein NIP5;1 is essential for efficient boron uptake and plant development under boron limitation. *The Plant Cell*, 18, 1498–1509. https://doi.org/10.1105/tpc.106.041640

Tarkowska, D., Filek, M., Biesaga-Koscielniak, J., Marcinska, I., Machackova, I., Krekule, J. et al. (2012) Cytokinins in shoot apices of *Brassica napus* plants during vernalization. *Plant Science*, 187, 105–112.

Warington, K. (1923) The effect of boric acid and borax on the broad bean and certain other plants. *Annals of Botany*, 37, 629–672.

Wimmer, M., Abreu, I., Bell, R., Bienert, M.D., Brown, P., Dell, B. et al. (2020) Boron: an essential element for vascular plants. *New Phytologist*, 226, 1232–1237.

Wingler, A. & Roitsch, T. (2008) Metabolic regulation of leaf senescence: interactions of sugar signalling with biotic and abiotic stress responses. *Plant Biology*, 10, 50–62.

Wolters, H. & Jurgens, G. (2009) Survival of the flexible: hormonal growth control and adaptation in plant development. *Nature Reviews Genetics*, 10, 305–317. https://doi.org/10.1038/nrg2558

Woo, J., MacPherson, C.R., Liu, J., Wang, H., Kiba, T., Hannah, M.A. et al. (2012) The response and recovery of the *Arabidopsis thaliana* transcriptome to phosphate starvation. *BMC Plant Biology*, 12, 62. https://doi.org/10.1186/1471-2229-12-62

Zhou, T., Hua, Y., Huang, Y., Ding, G., Shi, L. & Xu, F. (2016) Physiological and transcriptional analyses reveal differential phytohormone responses to boron deficiency in *Brassica napus* genotypes. *Frontiers in Plant Science*, 7, 221. https://doi.org/10.3389/fpls.2016.00221

Zierer, W., Hajirezaei, M.R., Eggert, K., Sauer, N., von Wirén, N. & Pommerrenig, B. (2016) Phloem-specific methionine recycling fuels polyamine biosynthesis in a sulfur-dependent manner and promotes flower and seed development. *Plant Physiology*, 170, 790–806. https://doi.org/10.1104/pp.15.00786

SUPPORTING INFORMATION

Additional supporting information can be found online in the Supporting Information section at the end of this article.

How to cite this article: Pommerrenig, B., Faber, M., Hajirezaei, M.-R., von Wirén, N. & Bienert, G.P. (2022) Cytokinins as boron deficiency signals to sustain shoot development in boron-efficient oilseed rape. *Physiologia Plantarum*, 174(5), e13776. Available from: https://doi.org/10.1111/ppl.13776